Bioelectrochemistry 88 (2012) 42–47

Contents lists available at SciVerse ScienceDirect

Bioelectrochemistry

journal homepage: www.elsevier.com/locate/bioelechem

# Electrochemical DNA biosensor with chitosan-$Co_3O_4$ nanorod-graphene composite for the sensitive detection of *staphylococcus aureus nuc* gene sequence

Xiaowei Qi [a,b], Hongwei Gao [c], Yuanyuan Zhang [b], Xiuzhen Wang [b], Ying Chen [d], Wei Sun [a,b,*]

[a] College of Chemistry and Chemical Engineering, Hainan Normal University, Haikou, 571158, P. R. China
[b] College of Chemistry and Molecular Engineering, Qingdao University of Science and Technology, Qingdao, 266042, P. R. China
[c] Shandong Entry-Exit Inspection and Quarantine Bureau of the People's Republic of China, Qingdao, 266002, P. R. China
[d] Chinese Academy of Inspection and Quarantine, Institute of Food Safety, Beijing, P. R. China

ARTICLE INFO

*Article history:*
Received 29 August 2011
Received in revised form 18 April 2012
Accepted 31 May 2012
Available online 11 June 2012

*Keywords:*
$Co_3O_4$ nanorod
Graphene
Chitosan
Carbon ionic liquid electrode
Electrochemical DNA biosensor

ABSTRACT

In this paper a novel nanocomposite material prepared by $Co_3O_4$ nanorods (nano-$Co_3O_4$), graphene (GR) and chitosan (CTS) was fabricated and further modified on carbon ionic liquid electrode (CILE), which was used as the substrate electrode to construct a new electrochemical DNA biosensor. The single-stranded DNA (ssDNA) probe was immobilized on the CTS–$Co_3O_4$–GR/CILE surface by electrostatic attraction, which could hybridize with the target ssDNA sequence under the selected conditions. By using methylene blue (MB) as the electrochemical indicator, the hybridization reactions were monitored with the reduction peak current. By combining the biocompatibility of $Co_3O_4$ nanorods, excellent electron transfer ability and big surface of GR, good film-forming ability of CTS and the high conductivity of CILE, the amount of ssDNA adsorbed on the electrode surface was increased and the electrochemical response of MB was accelerated. Under the optimal conditions differential pulse voltammetric responses of MB were in linear with the specific target ssDNA sequence in the concentration range from $1.0\times10^{-12}$ to $1.0\times10^{-6}$ M with the detection limit as $4.3\times10^{-13}$ M (3σ). Good discrimination ability to the one-base and three-base mismatched ssDNA sequences could be achieved and the polymerase chain reaction (PCR) amplification products of *Staphylococcus aureus nuc* gene sequence were detected with satisfactory results.



## 1. Introduction

Molecular diagnostics based on the analysis of special gene sequences have offered a highly sensitive and quantitative method for the detection of pathogenic microorganisms. Traditional DNA detection methods based on the coupling of electrophoresis separations and radio isotopic detection are labor intensive and time consuming. Among the different DNA hybridization assay method, electrochemical DNA biosensors have been greatly developed due to the high sensitivity, small dimensions, low cost, fast response, miniaturized and automated devices. Various kinds of modified electrodes have been devised for the ssDNA immobilization [1,2]. Among them, nanomaterials have been widely used with the advantages such as high surface area, favorable electronic properties and electrocatalytic activity as well as good biocompatibility enabled by their nanometer sizes. Mao et al. [3] reviewed the advances of different nanomaterials based electrochemical DNA biosensors. Bonanni et al. [4] reviewed the nanomaterial based DNA sensors with electrochemical impedance spectroscopy as the transduction technique.

$Co_3O_4$ is an important p-type metal oxide semiconductor with its potential applications in ceramic pigments, chemical sensors, energy storage, heterogeneous catalysts and electrochromic devices [5]. Dan et al. [6] electrodeposited $PbO_2$ and nano-$Co_3O_4$ on Ti substrate electrode and applied to the study of oxygen evolution reaction. Ding et al. [7] fabricated $Co_3O_4$ nanofibers by a two-step procedure consisting of electrospinning with subsequent calcinations and further applied it to construct a non-enzymatic sensor for glucose detection in alkaline solution. Lu et al. [8] synthesized layered $Co_3O_4$ nanoflakes with spongy nanostructure as an immobilization matrix to entrap hemoglobin.

As a new form of carbon, graphene (GR) is a single-atom thick, two dimensional sheet of $sp^2$ bonded carbon [9]. Due to its high mobility of charge carriers, high specific surface area, quantum hall effect and upstanding electric conductivity, GR is an ideal material for the construction of electrochemical sensors and biosensors [10–12], which exhibits excellent electrocatalytic activity and high adsorption ability [13]. For instance, Lim et al. [14] applied the epitaxial GR as an anode material for the simultaneous detection of all four DNA bases in double stranded DNA (dsDNA) without a prehydrolysis step. Li applied GR modified electrode towards the electrocatalytic oxidation of dopamine and methanol [15,16]. In addition GR can provide a favorable microenvironment for DNA and effectively accelerate the

* Corresponding author at: College of Chemistry and Molecular Engineering, Qingdao University of Science and Technology, Qingdao, 266042, P. R. China. Fax: +86 532 84023927.
*E-mail address:* sunwei@qust.edu.cn (W. Sun).

1567-5394/$ – see front matter © 2012 Elsevier B.V. All rights reserved.
doi:10.1016/j.bioelechem.2012.05.007

direct electron transfer rate from DNA to the electrode surface, which can be further applied to determine DNA with excellent sensitivity and long-term stability [17,18].

Carbon ionic liquid electrode (CILE) is a new kind of working electrode prepared with ionic liquid (IL) as a binder and a modifier. CILE has been exhibited many advantages such as wide electrochemical windows, inherent electrocatalytic ability and anti-fouling ability due to the addition of ILs, which has the specific properties such as high chemical and thermal stability, negligible vapor pressure, high ionic conductivity, wide electrochemical windows [19]. Different kinds of CILE had been fabricated and applied to the electrochemical detection of electroactive molecules. Shiddiky and Torriero [20] reviewed electrochemical biosensors based on CILEs or IL/composite modified electrodes. Safavi et al. [21] utilized octylpyridinium hexafluorophosphate as the binder to make a CILE for the electrochemical detection. Sun et al. applied the CILEs as the basal electrode for the redox protein electrochemistry with different nanoparticles such as ZnO nanoparticles [22] and CdS nanorods [23].

In this paper a CILE was fabricated by using 1-butylpyridinium hexafluorophosphate ($BPPF_6$) as binder and modifier, which was further used as the basal electrode for the fabrication of electrochemical DNA biosensor. Then $Co_3O_4$ nanorods (nano-$Co_3O_4$), graphene (GR) and chitosan (CTS) were mixed together to form a novel nanocomposite material and casted on the surface of CILE. To the best of our knowledge, the usage of CTS–$Co_3O_4$–GR nanocomposite matrix as the DNA immobilization platform for the enlargement of the electrochemical signal and the increase of the sensitivity for DNA detection has not been reported previously. The nanocomposite film has a very large surface area, good conductivity and excellent porous structure, which lead to the measurable currents even for low concentrations of ssDNA sequence. The proposed electrochemical DNA sensor was applied to the detection of *nuc* gene sequence fragment from the *Staphylococcus aureus* and further used to the PCR product of *Staphylococcus aureus* endogenous gene, which exhibited the advantages such as the simple preparation procedure, high selectivity and broad linear range.

## 2. Experimental

### 2.1. Apparatus and chemicals

All the electrochemical experiments were performed on a CHI 750B electrochemical workstation (Shanghai CH Instruments, China). A three-electrode system was employed for the electrochemical investigation, which was composed of a nanocomposite modified CILE as working electrode, a Pt wire as auxiliary electrode and a saturated calomel electrode (SCE) as reference electrode. Scanning electron microscope (SEM) images were obtained by a JSM-6700F scanning electron microscope (Japan Electron Company, Japan). The PCR amplification was performed on an Eppendorf Mastercycler Gradient PCR system (Eppendorf, Germany).

1-Butylpyridinium hexafluorophosphate ($BPPF_6$, >99%, Lanzhou Greenchem and Catalysis, ILS., LICP., CAS., China), chitosan (CTS, minimum 92% deacetylated, Dalian Xindie Co. Ltd., China), graphite powder (average particle size 30 μm, Shanghai Colloid Chemical Co. Ltd., China) and methylene blue (MB, Shanghai Chemicals Plant, China) were used as received. Graphene (GR) and $Co_3O_4$ nanorods were synthesized by the modified Hummer's method [24,25] and hydrothermal method [26], respectively. Solutions for PCR experiments, such as 10× reaction buffer B (Promega, Wisconsin, USA), Taq DNA polymerase (Promega, Wisconsin USA), 1× TAE buffer (40.0 mM Tris, 1.0 mM EDTA, 40.0 mM acetate, pH 8.0), 50.0 mM Tris–HCl buffer solution (pH 7.0), 50.0 mM phosphate-buffered solution (PBS, pH = 7.0), were prepared as usual. All the solutions were prepared with doubly distilled water and all the experiments were achieved at room temperature unless special indicated.

The 22-base oligonucleotides probe (probe ssDNA), target complementary sequence DNA (target ssDNA), one-base mismatched ssDNA, three-base mismatched ssDNA and noncomplementary sequence DNA (ncDNA) were synthesized by Shanghai Sangon Biological Engineering Technological Co. Ltd. (China), which were related to the *nuc* gene sequence of *Staphylococcus aureus*. Their base sequences were list as below:

probe ssDNA: 5′-TGG ACG TGG CTT AGC GTA TAT T-3′;
target ssDNA: 5′-AAT ATA CGC TAA GCC ACG TCC A-3′;
one-base mismatched ssDNA: 5′-AAG ATA CGC TAA GCC ACG TCC A-3′;
three-base mismatched ssDNA: 5′-AAG ATA CGC TAC GCC ACG TCT A-3′;
noncomplementary ssDNA (ncDNA):5′-ACC GGT AGC GTT GCC AGC TTC G-3′.

The DNA sample for PCR amplification was extracted from *staphylococcus aureus* strains. The PCR reaction was performed on an Eppendorf Mastercycler Gradient PCR system using oligonucleotide primers for *nuc* gene of *staphylococcus aureus* with the following sequences:

Primer F: 5′-CCT GAA GCA AGT GCA TTT ACG A-3′;
Primer R: 5′-CTT TAG CCA AGC CTT GAC GAA CT-3′.

### 2.2. Preparation of the modified electrode

Carbon ionic liquid electrode (CILE) was fabricated based on the reference [27]. 3.0 g of graphite powder and 1.0 g of $BPPF_6$ were mixed thoroughly in a mortar and further heated at 80 °C to form a homogeneous carbon paste. A portion of the carbon paste was filled into one end of a glass tube (Φ = 4 mm) and a copper wire was inserted to establish an electrical contact. The surface of CILE was smoothed on a piece of weighing paper just before use.

The nanocomposite was prepared by dispersing 0.2 mg/mL of $Co_3O_4$ nanorods and 0.8 mg/mL of GR in 1.0 mg/mL CTS (in 1.0% HAc solution) and sonicated for 30 min to get a homogeneous solution. Then, 7.0 μL of the prepared CTS–$Co_3O_4$–GR suspension solution was dropped onto the fresh prepared surface of the CILE and naturally dried in the air to form the modified electrode, which was denoted as CTS–$Co_3O_4$–GR/CILE. Other electrodes were prepared by the same procedure as the comparative experiments.

### 2.3. Fabrication of electrochemical DNA biosensor

Immobilization of ssDNA probes was performed by dropping 10.0 μL of $1.0\times10^{-6}$ M probe ssDNA (in 50.0 mM pH 7.0 PBS) directly onto the surface of CTS–$Co_3O_4$–GR/CILE. The oligonucleotide probe was immobilized by the electrostatic adsorption of negative charged ssDNA molecules on the positive charged CTS film [28]. At the same time, the presence of $Co_3O_4$-GR nanocomposite material can provide more adsorption sites and biocompatible microenvironment for the probe ssDNA with the increase of the surface area. Then the electrode was washed with 0.5% sodium dodecyl sulfate (SDS) solution and doubly distilled water for 3 times successively to remove unabsorbed probe ssDNA on the surface of electrode. This probe-captured electrode was denoted as ssDNA/CTS–$Co_3O_4$–GR/CILE.

The efficient drop hybridization procedure was further used for the target ssDNA sequence hybridized with the probe ssDNA modified electrode [29,30], which was performed by dropping 5.0 μL target ssDNA sequence (in 50.0 mM PBS) directly onto the ssDNA/CTS–$Co_3O_4$–GR/CILE surface, which was inverted upside down to hold the solution. The hybridization between the target sequence and the probe sequence was allowed to proceed for 20 min at room temperature. During this procedure a small beaker was fit tightly over the electrode to prevent the quickly evaporation of the ssDNA solution

with the completely hybridization. Then the electrode was washed with 0.5% SDS solution and doubly distilled water for 3 times to remove the unhybridized target ssDNA sequence. This hybridized electrode was further named as dsDNA/CTS–$Co_3O_4$–GR/CILE.

### 2.4. Electrochemical detection

The dsDNA/CTS–$Co_3O_4$–GR/CILE was immersed into $2.0\times10^{-5}$ M MB solution for 10 min to accumulate the electrochemical indicator (MB) and then washed with 50.0 mM PBS for 3 times. The cathodic response of the accumulated MB on the electrode surface was measured by the sensitive differential pulse voltammetry (DPV) in a 50.0 mM Tris–HCl buffer solution (pH 7.0) with instrumental parameters as: pulse amplitude 0.008 V, pulse width 0.05 s and pulse period 0.2 s.

Electrochemical impedance spectroscopy (EIS) was carried out in a 1.0 mM $[Fe(CN)_6]^{3-/4-}$ solution containing 0.1 M KCl with the frequencies swept from $10^4$ to 0.1 Hz.

### 2.5. Polymerase chain reaction of staphylococcus aureus nuc gene sequence

Amplification of *nuc* gene fragments was carried out in a final volume of 25 μL in 0.2 mL tube containing 200.0 nM each primer of *nuc* primer F and *nuc* primer R, 10× reaction buffer B, 2.0 mM $MgCl_2$, 200.0 nM each of dATP, dCTP, dGTP and dTTP; 1.5 units of Taq DNA polymerase, 1.0 μL DNA template purified from samples. During the PCR procedure, DNA was initial denatured at 94 °C for 30 s. PCR conditions were optimized as follows: 35 cycles of amplification (94 °C for 30 s, 56 °C for 30 s, 72 °C for 30 s) and final extension at 72 °C for 5 min. The PCR products without DNA template were used as comparison and the PCR products were kept at 4 °C before use.

## 3. Results and discussion

### 3.1. Scanning electron microscopic images of the nanomaterials

The scanning electron microscopic (SEM) images of the synthesized nanomaterials were recorded with the results shown in Fig. 1. As shown in Fig. 1A, rod-like nanostructures of $Co_3O_4$ appeared with the length of 500 nm and the diameter of 70 nm. Fig. 1B showed the typical ultrathin sheets and wrinkles of GR. This wrinkled nature of GR is highly beneficial in maintaining a high surface area on the electrode since the sheets cannot readily collapse back to a graphitic structure. By mixing $Co_3O_4$ nanorods with GR together and sonicating for 20 min, the image of $Co_3O_4$-GR nanocomposite was shown in Fig. 1C. It can be seen that $Co_3O_4$ nanorods were inserted into the layer of GR nanosheet and enlarged its layer distances, which could provide an increased roughness of the electrode surface with better biocompatibility. The high surface area is helpful in the loading of probe ssDNA on the surface. The excellent conductivity and small band gap of GR are favorable for conducting electrons from the biomolecules [14]. GR-based electrochemical sensors can also exhibit a much higher sensitivity because of the low electronic noise from thermal effect.

### 3.2. Electrochemical impedance spectra of the modified electrodes

Electrochemical impedance spectroscopy (EIS) is a powerful method to analyze the complex electrical resistance of a system and is sensitive to surface phenomena and changes of bulk properties. Different nanomaterials modified electrodes were characterized by EIS and the semicircle portion observed at high frequencies in the Nyquist diagrams corresponded to the electron transfer limiting process. The interfacial electron transfer resistance (Ret) can be calculated from the diameter of Nyquist diagram, which was performed in 1.0 mM $[Fe(CN)_6]^{3-/4-}$ solution with the frequencies swept from $10^4$ to 0.1 Hz. As illustrated in Fig. 2, the Ret value of CILE was got as 163.7 Ω (curve a). On the CTS–$Co_3O_4$/CILE and CTS–GR/CILE the Ret values decreased to 96.4 Ω (curve b) and 64.6 Ω (curve c) respectively, indicating the presence of $Co_3O_4$ nanorods or GR nanosheets on the electrode surface could obviously improve the electron transfer rate of ferricyanide. Also the conductivity of GR was higher than that of $Co_3O_4$ nanorods, which resulted in the smaller Ret value on the GR modified electrode. On CTS–$Co_3O_4$–GR/CILE (curve d) the Ret value was further decreased to 27.4 Ω, indicating the highest conductivity of the electrode interface with the composite material. So the synergistic effects of $Co_3O_4$-GR nanomaterial in the film greatly enhanced the electron transfer rate of $[Fe(CN)_6]^{3-/4-}$ and decreased the interface resistance, which could act as an excellent platform for electrode modification.

### 3.3. Differential pulse voltammogram of MB at different modified electrodes

MB is a commonly used electrochemical indicator in the DNA biosensor, which can distinguish the ssDNA and dsDNA sequences [31]. MB can exhibit different interaction models with ssDNA and dsDNA such as electrostatic binding and intercalation with the major or minor grooves of dsDNA helix. Yang et al. reported the specific interaction of MB with guanine bases in DNA sequence [32]. The interaction may be related to different experimental conditions such as the DNA sequences, ion strength, MB concentration and buffer pH, which results in the higher affinity of dsDNA with MB and can be used to distinguish the dsDNA and ssDNA [33,34]. Fig. 3 showed the differential pulse voltammograms of $2.0\times10^{-5}$ M MB on CTS–$Co_3O_4$–GR/CILE (curve a), ssDNA/CTS–$Co_3O_4$–GR/CILE (curve b), dsDNA/CTS/CILE (curve c), dsDNA/CTS–$Co_3O_4$/CILE (curve d), dsDNA/CTS–GR/CILE (curve e) and dsDNA/CTS–$Co_3O_4$–GR/CILE (curve f) in 50.0 mM Tris–HCl buffer solution. On the CTS–$Co_3O_4$–GR/CILE (curve a) the smallest peak current of MB appeared. With the immobilization of ssDNA on the modified electrode, the reduction peak current increased a little (curve b), indicating that the small amount of MB was adsorbed on the electrode surface due to its interaction with ssDNA by electrostatic attraction. While on the dsDNA modified electrode the reduction peak current increased

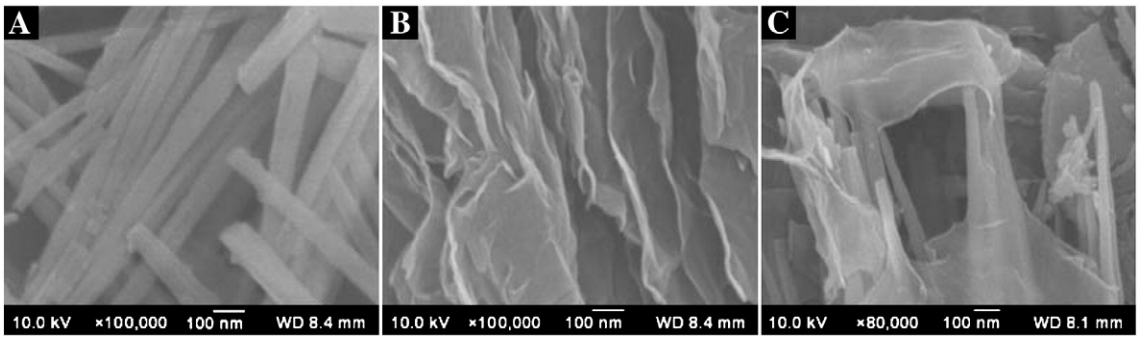


**Fig. 1.** SEM images of the $Co_3O_4$ nanorods (A), GR (B) and $Co_3O_4$–GR composite (C).

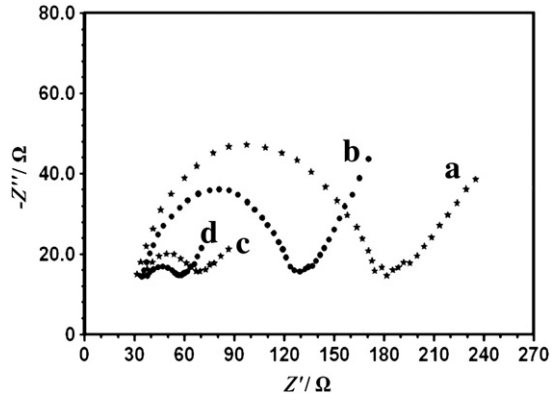


**Fig. 2.** Electrochemical impedance spectra of different modified electrodes in 1.0 mM $[Fe(CN)_6]^{3-/4-}$ containing 0.1 M KCl (from a to d were CILE, CTS–$Co_3O_4$/CILE, CTS–GR/CILE and CTS–$Co_3O_4$–GR/CILE, respectively) with the frequency swept from $10^4$ to 0.1 Hz.

greatly, which can be attributed to the strong intercalation between MB and dsDNA (curves c to f). Also the reduction peak current of MB increased gradually with the step-by-step incorporation of nanomaterials in the film, indicating the amount of dsDNA on the electrode surface was increased. The results were attributed to the gradually increase of the electrode effective area, which could provide more sites for the immobilization of dsDNA on the electrode surface, and further accumulate more MB molecules on the electrode surface, then the reduction peak current of MB was increased. The largest reduction peak current appeared on the dsDNA/CTS–$Co_3O_4$–GR/CILE, indicating that the biggest amounts of dsDNA present on the electrode surface could interact with more MB molecules. The above results confirmed that the synergetic effects of $Co_3O_4$ nanorods and GR in the nanocomposite film could effectively enhance the surface concentrations of dsDNA due to the large surface area and roughness of the electrode interface.

### 3.4. Optimization of the electrode preparation

The ratio of $Co_3O_4$ nanorods and GR in the nanocomposite influenced the electron transfer rate of MB and the maximum loading amount of ssDNA probe on the electrode surface. Different mass ratios of $Co_3O_4$ nanorods and GR such as 9:1, 8:2, 7:3, 6:4, 1:1, 4:6, 3:7, 2:8 and 1:9 were studied. When the proportion of $Co_3O_4$ nanorods was too small, the immobilization amount of ssDNA probes was limited. When the quantity of $Co_3O_4$ nanorods was too large, the conductivity of the nanocomposite membrane modified electrode decreased obviously due to the semiconductivity of $Co_3O_4$ nanomaterials. Therefore, the mixture of 0.2 mg $Co_3O_4$ nanorods and 0.8 mg GR dispersed in 1.0 mL of 1.0 mg/mL CTS (in 1.0% HAc solution) was chosen in experiments.

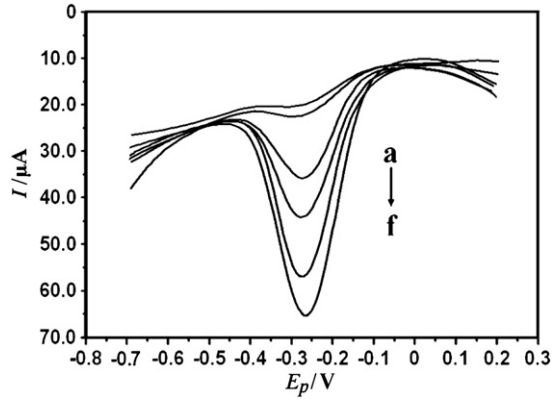


**Fig. 3.** Differential pulse voltammograms of (a) CTS–$Co_3O_4$–GR/CILE, (b) ssDNA/CTS–$Co_3O_4$–GR/CILE, (c) dsDNA/CTS/CILE, (d) dsDNA/CTS–$Co_3O_4$/CILE, (e) dsDNA/CTS–GR/CILE and (f) dsDNA/CTS–$Co_3O_4$–GR/CILE with a $2.0\times10^{-5}$ M MB in 50.0 mM Tris–HCl buffer solution (pH 7.0).

### 3.5. Effect of concentration and accumulation time of MB

The concentration and accumulation time of hybridization indicator can influence the performance of the prepared DNA biosensor. In order to maximize the efficiency and sensitivity of the DNA biosensor, the experimental conditions were optimized with the results shown in Fig. 4. The current response increased with the MB concentration from $2.0\times10^{-6}$ to $6.0\times10^{-5}$ M and intended to be stable at the concentration of $2.0\times10^{-5}$ M or above (Fig. 4A). Therefore, $2.0\times10^{-5}$ M of MB was employed as the indicator. Accumulation time of MB on the electrode surface was further investigated. The highest current signal of MB was obtained after 10 min accumulation and a signal plateau appeared when the accumulation time exceeded 10 min (Fig. 4B). So 10 min was chosen as the optimal accumulation time.

### 3.6. Selectivity of the electrochemical DNA biosensor

The selectivity was investigated by using ssDNA/CTS–$Co_3O_4$–GR/CILE to hybridize with different ssDNA sequences related to *nuc* gene of *staphylococcus aureus*. Fig. 5 showed the reductive peak of MB on different DNA modified electrodes such as the probe ssDNA modified electrode (curve a) and after hybridization with the noncomplementary ssDNA sequence (curve b), three-base mismatched ssDNA sequence (curve c), one-base mismatched ssDNA sequence (curve d) and the complementary ssDNA sequence (curve e). The biggest reduction peak current (55.2 μA) was obtained after hybridized with the complementary ssDNA sequence (curve e), indicating the formation of hybridized dsDNA molecules on the electrode surface could accumulate the biggest amounts of MB molecules. The reduction peak current of MB was got as 10.1 μA after hybridized with the noncomplementary ssDNA (curve b), which may be attributed to the non-specific adsorption of ssDNA on the electrode surface. After the probe ssDNA was hybridized with the three-base mismatched ssDNA (curve c) and one-base mismatched ssDNA (curve d), the reductive peak currents increased to 25.7 and 41.9 μA, respectively. Also the bigger response appeared on the one-base mismatched ssDNA than that of the three-base mismatched ssDNA. The results demonstrated that the fabricated DNA biosensor exhibited high selectivity and good distinguish ability for the hybridization detection of different ssDNA sequences.

### 3.7. Calibration curve

Under the optimal conditions this electrochemical DNA biosensor was hybridized with different concentrations of target ssDNA sequence related to *nuc* gene sequence by the experimental procedure and the reductive peak current of MB was measured. The peak current of MB increased gradually with the increase of the target ssDNA concentration and the typical differential pulse voltammograms were shown in

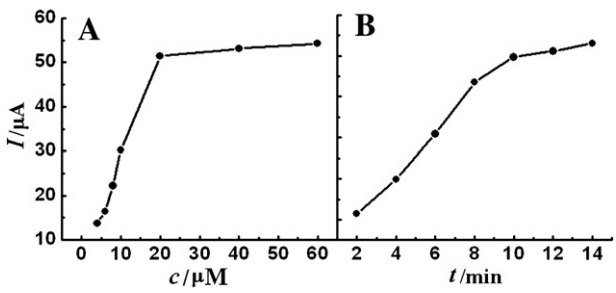


**Fig. 4.** Optimization of concentration (A) and accumulation time (b) of MB.

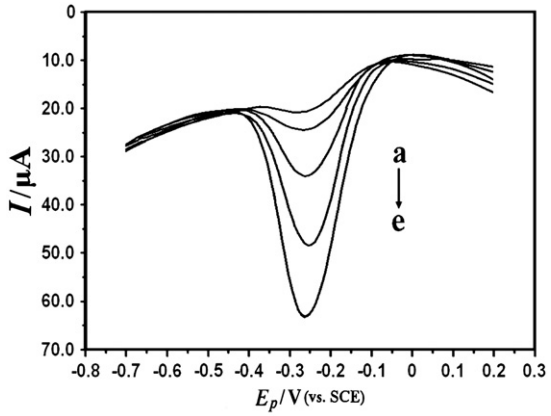


**Fig. 5.** Differential pulse voltammograms of $2.0\times10^{-5}$ M MB at the probe ssDNA modified electrode (a) and after hybridization with the noncomplementary ssDNA sequence (b), three-base mismatched ssDNA sequence (c), one-base mismatched ssDNA sequence (d) and the complementary ssDNA sequence (e).

Fig. 6. The differences of MB reductive peak current before and after the hybridization was linear with the logarithmic value of the *nuc* gene ssDNA sequence concentration in the range from $1.0\times10^{-12}$ M to $1.0\times10^{-6}$ M with a correlation coefficient of 0.998 and the linear regression equation of $\Delta I(\mu A) = 6.96\log[c/(M)] + 97.7$ ($n=7$, $\gamma=0.994$) (where $c$ is the concentration of *staphylococcus aureus nuc* gene sequence; $\Delta I$ is the difference of MB peak current before and after hybridization). A detection limit of the *staphylococcus aureus nuc* gene sequence was estimated to be $4.3\times10^{-13}$ M ($3\sigma$) (where $\sigma$ is the relative standard deviation of the blank solution, $n=11$). The relation standard deviation (RSD) for the detection of $1.0\times10^{-7}$ M target ssDNA sequence was 3.7%, indicating the good reproducibility of this measurement.

### 3.8. Detection of PCR product of staphylococcus aureus nuc gene

The PCR amplified product of *staphylococcus aureus nuc* gene was further detected by this electrochemical DNA biosensor under the selected conditions. The template DNA for PCR amplification was extracted from *staphylococcus aureus* strains and amplified based on the previous mentioned PCR conditions. The PCR amplified samples were analyzed by agarose gel electrophoresis separation with ethidium bromide for DNA staining and visualized with UV transilluminator, which gave a final gene fragment length of 166 bp. The obtained product was diluted with 50.0 mM PBS buffer solution (pH 7.0), denatured by heating it in boiling water bath for 10 min and frozen in an ice bath for 2 min. Then 5.0 μL of the denatured PCR amplification product was dropped directly onto ssDNA/CTS–$Co_3O_4$–GR/CILE for hybridization. After hybridization, the electrode was immersed into MB solution for the detection based on the experimental procedure with the results shown in Fig. 7. An increase of the reduction peak current appeared after hybridized with the denatured PCR amplified sample of *nuc* gene (curve c), which was much larger than hybridized with that of PCR solution without DNA template (curve b), indicating the PCR experiment was proceeded smoothly and target ssDNA sequences were successfully amplified. The increase of the reduction peak current on the curve b compared with the MB signal at the ssDNA/CTS–$Co_3O_4$–GR/CILE (curve a) may be caused by the non-specific adsorption effect. The obvious increase of the reduction peak current on curve c indicated the successful accomplishment of the hybridization reaction on the electrode surface, which resulted in the formation of dsDNA with more MB molecules accumulated. This significant differences of the MB signals between the probe ssDNA modified electrode and the hybridized dsDNA modified electrode confirmed the good selectivity of this constructed DNA biosensor, which could be further applied to the effectively detection of the *staphylococcus aureus nuc* gene sequence in PCR amplified samples.

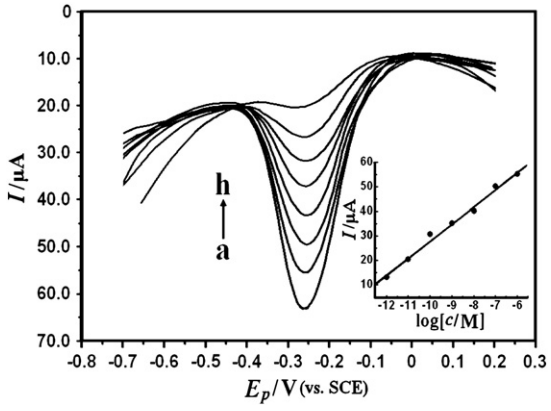


**Fig. 6.** Differential pulse voltammograms of MB on ssDNA/CTS–$Co_3O_4$–GR/CILE after hybridization with target ssDNA sequences (from a to h were $1.0\times10^{-6}$, $1.0\times10^{-7}$, $1.0\times10^{-8}$, $1.0\times10^{-9}$, $1.0\times10^{-10}$, $1.0\times10^{-11}$, $1.0\times10^{-12}$ and 0 M). Insert: plots of I versus logarithm of target ssDNA concentration.

## 4. Conclusions

A CTS–$Co_3O_4$–GR nanocomposite film modified CILE was fabricated and further characterized by scanning electron microscope and electrochemical impedance spectroscopy. Due to the presence of $Co_3O_4$ nanorods and GR nanosheets on the electrode surface, effective surface area and electron conductivity were greatly increased. Based on the nanocomposite modified electrode, ssDNA was further immobilized on the electrode surface to get a new electrochemical DNA sensor, which was further applied to the detection of *staphylococcus aureus nuc* gene and its PCR products. The loading amount of probe ssDNA sequences were improved by synergistic effects of nanomaterials, which further improved the detection sensitivity for target ssDNA hybridization. The detection of the *nuc* gene sequence can be achieved in the concentration range from $1.0\times10^{-12}$ to $1.0\times10^{-6}$ M with the detection limit of $4.3\times10^{-13}$ M ($3\sigma$). The electrochemical DNA sensor exhibited the advantages such as simple preparation procedure, low cost, fast response, good selectivity, wide linear and high sensitivity, which provided a potential platform for the construction of other electrochemical sensors.

## Acknowledgements

We acknowledge the financial support of the National Natural Science Foundation of China (no. 21075071), the project of Chinese Academy of Inspection and Quarantine (Jianke2009jk009), National

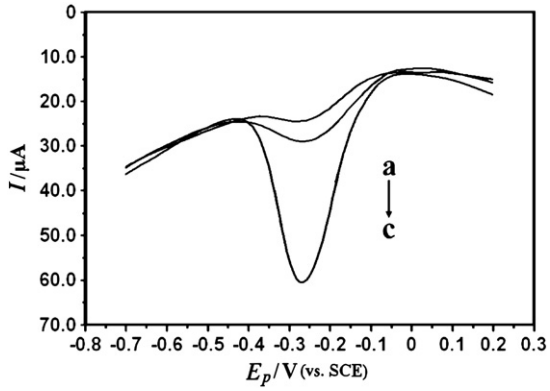


**Fig. 7.** Differential pulse voltammograms of MB on ssDNA/CTS–$Co_3O_4$–GR/CILE (a), and hybridized with the PCR product without (b) and with (c) DNA template of *Staphylococcus aureus nuc* gene.

Department Public Benefit Research Foundation (201110015) and the Shandong Province Natural Science Foundation (ZR2009BL017).

## References


[1] K. Xu, J.R. Huang, Z.Z. Ye, Y.B. Ying, Y.B. Li, Recent development of nanomaterials used in DNA biosensors, Sensors 9 (2009) 5534–5557.
[2] F.R.R. Teles, L.P. Fonseca, Trends in DNA biosensors, Talanta 77 (2008) 606–623.
[3] X. Mao, G.D. Liu, Nanomaterial based electrochemical DNA biosensors and bioassays, J. Biomed. Nanotechnol. 4 (2008) 419–431.
[4] A. Bonanni, M. del Valle, Use of nanomaterials for impedimetric DNA sensors: a review, Anal. Chim. Acta 678 (2010) 7–17.
[5] E. Hosono, S. Fujihara, I. Honmaa, H.S. Zhou, Fabrication of morphology and crystal structure controlled nanorod and nanosheet cobalt hydroxide based on the difference of oxygen-solubility between water and methanol, and conversion into $Co_3O_4$, J. Mater. Chem. 15 (2005) 1938–1945.
[6] Y.Y. Dan, H.Y. Lu, X.L. Liu, H.B. Lin, J.Z. Zhao, Ti/$PbO_2$ + nano-$Co_3O_4$ composite electrode material for electrocatalysis of $O_2$ evolution in alkaline solution, Int. J. Hydrogen Energy 36 (2011) 1949–1954.
[7] Y. Ding, Y. Wang, L. Su, M. Bellagamba, H. Zhang, Y. Lei, Electrospun $Co_3O_4$ nanofibers for sensitive and selective glucose detection, Biosens. Bioelectron. 26 (2010) 542–548.
[8] X.B. Lu, G.F. Zou, J.H. Li, Hemoglobin entrapped within a layered spongy $Co_3O_4$ based nanocomposite featuring direct electron transfer and peroxidase activity, J. Mater. Chem. 17 (2007) 1427–1432.
[9] E. Stolyarova, K.T. Rim, S. Ryu, J. Maultzsch, P. Kim, L.E. Brus, T.F. Heinz, M.S. Hybertsen, G.W. Flynn, High-resolution scanning tunneling microscopy imaging of mesoscopic graphene sheets on an insulating surface, Proc. Natl. Acad. Sci. U. S. A. 104 (2007) 9209–9212.
[10] A.K. Geim, K.S. Novoselov, The rise of graphene, Nat. Mater. 6 (2007) 183–191.
[11] D. Li, M.B. Müller, S. Gilje, R.B. Kaner, G.G. Wallace, Processable aqueous dispersions of graphene nanosheets, Nat. Nanotechnol. 3 (2008) 101–105.
[12] S. Park, R.S. Ruoff, Chemical methods for the production of graphenes, Nat. Nanotechnol. 4 (2009) 217–224.
[13] M. Pumera, A. Ambrosi, A. Bonanni, E.L.K. Chng, H.L. Poh, Graphene for electrochemical sensing and biosensing, Trends Anal. Chem. 29 (2010) 954–965.
[14] C.X. Lim, H.Y. Hoh, P.K. Ang, K.P. Loh, Direct voltammetric detection of DNA and pH sensing on epitaxial graphene: an insight into the role of oxygenated defects, Anal. Chem. 82 (2010) 7387–7393.
[15] Y. Wang, Y. Li, L. Tang, J. Lu, J. Li, Application of graphene-modified electrode for selective detection of dopamine, Electrochem. Commun. 11 (2009) 889–892.
[16] Y. Li, L. Tang, J. Li, Preparation and electrochemical performance for methanol oxidation of pt/graphene nanocomposites, Electrochem. Commun. 11 (2009) 846–849.
[17] S. Stankovich, D.A. Dikin, G.H.B. Dommett, K.M. Kohlhaas, E.J. Zimney, E.A. Stach, R.D. Piner, S.T. Nguyen, R.S. Ruoff, Graphene-based composite materials, Nature 442 (2006) 282–286.
[18] H.W.Ch. Postma, Rapid sequencing of individual DNA molecules in graphene nanogaps, Nano Lett. 10 (2010) 420–425.
[19] S. Pandey, Analytical applications of room-temperature ionic liquids: a review of recent efforts, Anal. Chim. Acta 556 (2006) 38–45.
[20] M.J.A. Shiddiky, A.A.J. Torriero, Application of ionic liquids in electrochemical sensing systems, Biosens. Bioelectron. 26 (2011) 1775–1787.
[21] A. Safavi, N. Maleki, O. Moradlou, M. Sorouri, Direct electrochemistry of hemoglobin and its electrocatalytic effect based on its direct immobilization on carbon ionic liquid electrode, Electrochem. Commun. 10 (2008) 420–423.
[22] W. Sun, Z.Q. Zhai, D.D. Wang, S.F. Liu, K. Jiao, Electrochemistry of hemoglobin entrapped in a Nafion/nano-ZnO film on carbon ionic liquid electrode, Bioelectrochemistry 74 (2009) 295–300.
[23] W. Sun, D.D. Wang, K. Jiao, Direct electron transfer of hemoglobin in a CdS nanorods and Nafion composite film on carbon ionic liquid electrode, Electrochim. Acta 53 (2008) 8217–8221.
[24] W.S. Hummers Jr., R.E. Offeman, Preparation of graphitic oxide, J. Am. Chem. Soc. 80 (1958) 1339.
[25] N.I. Kovtyukhova, P.J. Ollivier, B.R. Martin, T.E. Mallouk, S.A. Chizhik, E.V. Buzaneva, A.D. Gorchinskiy, Layer-by-layer assembly of ultrathin composite films from micron-sized graphite oxide sheets and polycations, Chem. Mater. 11 (1999) 771–778.
[26] J. Jiang, J.P. Liu, X.T. Huang, Y.Y. Li, R.M. Ding, X.X. Ji, Y.Y. Hu, Q.B. Chi, Z.H. Zhu, General synthesis of large-scale arrays of one-dimensional nanostructured $Co_3O_4$ directly on heterogeneous substrates, Cryst. Growth Des. 10 (2010) 70–75.
[27] W. Sun, M.X. Yang, R.F. Gao, K. Jiao, Electrochemical determination of ascorbic acid in room temperature ionic liquid $BPPF_6$ modified carbon paste electrode, Electroanalysis 19 (2007) 1597–1602.
[28] C. Xu, H. Cai, Q. Xu, P. He, Y. Fang, Characterization of single-stranded DNA on chitosan-modified electrode and its application to the sequence-specific DNA detection, Fresenius J. Anal. Chem. 369 (2001) 428–432.
[29] M.S. Hejazi, M.H. Pournaghi-Azar, E. Alipour, F. Karimi, Construction, electrochemically biosensing and discrimination of recombinant plasmid (pEThIL-2) on the basis of interleukine-2 DNA insert, Biosens. Bioelectron. 23 (2008) 1588–1594.
[30] M.H. Pournaghi-Azar, E. Alipour, S. Zununi, H. Froohandeh, M.S. Hejazi, Direct and rapid electrochemical biosensing of the human interleukin-2 DNA in unpurified polymerase chain reaction (PCR)-amplified real samples, Biosens. Bioelectron. 24 (2008) 524–530.
[31] T.G. Drummond, M.G. Hill, J.K. Barton, Electrochemical DNA sensors, Nat. Biotechnol. 21 (2003) 1192–1199.
[32] W.R. Yang, M. Ozsoz, D.B. Hibbert, J.J. Gooding, Evidence for the direct interaction between methylene blue and guanine bases using DNA-modified carbon paste electrodes, Electroanalysis 14 (2002) 1299–1302.
[33] J.Y. Gu, X.J. Lu, H.X. Ju, DNA sensor for recognition of native yeast DNA sequence with methylene blue as an electrochemical hybridization indicator, Electroanalysis 14 (2002) 949–954.
[34] S.O. Kelley, J.K. Barton, Electrochemistry of methylene blue bound to a DNA-modified electrode, Bioconjug. Chem. 8 (1997) 31–37.



**Xiaowei Qi** is now a master candidate in College of Chemistry and Molecular Engineering, Qingdao University of Science and Technology. He majors in modified electrode and electrochemical biosensors.

**Hongwei Gao** is a senior engineer in Agricultural Products Testing Center, Shandong Entry-Exit Inspection and Quarantine Bureau of People's Republic of China. She received her PhD in biotechnology from Institute of Oceanology, Chinese Academy of Science in 2008. Her current interests are bioengineering.

**Yuanyuan Zhang** is now a master candidate in College of Chemistry and Molecular Engineering, Qingdao University of Science and Technology. She majors in electrochemical DNA biosensors.

**Xiuzhen Wang** is now a master candidate in College of Chemistry and Molecular Engineering, Qingdao University of Science and Technology. He majors in nanoelectrochemical.

**Ying Chen** is a senior engineer in Institute of Food Safety, Chinese Academy of Inspection and Quarantine. Her current interests are bioengineering.

**Wei Sun** is a professor in College of Chemistry and Molecular Engineering, Qingdao University of Science and Technology. He received his PhD in analytical chemistry from Ocean University of China in 2002. His current interests are bioelectroanalysis.